ATLANTIS PRESS

Advances in Engineering Research, volume 110

3rd Annual International Conference on Advanced Material Engineering (AME 2017)

Two-Step Fabrication of Porous α-Fe_2O_3@TiO_2 core-shell Nanostructures with Enhanced Photocatalytic Activity

Xiao-Hong YANG[a], Shi-Yu SUN[b], Hai-Tao FU[*,c], Wu-Fa LI and Xi-Zhong AN[d]

School of Metallurgy, Northeastern University, Shenyang 110819, China

fuht@smm.neu.edu.cn

*Corresponding author

Keywords: α-Fe_2O_3 nanorods, TiO_2, Core-shell nanostructure, Photocatalysis

Abstract. A new synthetic approach has been developed to prepare α-Fe_2O_3@TiO_2 core-shell nanostructures at ambient conditions (e.g., in water, ≤100 °C). This approach shows a few unique features, including: short reaction time (a few minutes) for forming core-shell nanostructures, no requirement of high temperature calcinations for generating TiO_2 (e.g., at 80-100 °C), tunable TiO_2 shell thickness, high yield and good reproducibility. The experimental results show that the α-Fe_2O_3@TiO_2 core-shell nanostructures exhibit enhanced photocatalytic activity compared to the pure TiO_2 (P25) and pure Fe_2O_3 in degradation of organic dye molecules with visible light irradiation. This could be attributed to the large surface area of TiO_2 nanoparticles for maximum adsorption of dye molecules, and the effective charge separation at the heterojunction of α-Fe_2O_3 and TiO_2. The findings may open a new strategy to synthesize TiO_2-based photocatalysts with enhanced efficiency for environmental remediation applications.

Introduction

The design and fabrication of core-shell nanoparticles have attracted much more attention because of their unique shape, size and structure-dependent properties [1, 2]. The synergetic effects between the core and shell materials may drastically improve the overall performance of the hybrid composites, which results in a range of potential applications, including biomedical application [3, 4], catalysis [5, 6], electronics [7] and chemical sensors [8]. The properties of core-shell nanostructures can be adjusted by changing either the constituting materials or the core to shell ratio [9].

Among the well-known semiconductors, titanium oxide (TiO_2) nanoparticles have been regarded as one of the most promising nanomaterials because of its abundance, low-cost, long-term stability and nontoxicity [10]. In particular, TiO_2 coating on different metals or metal oxide nanoparticles as TiO_2-based core-shell nanocomposites have shown high potential research interests [11]. However, the photocatalytic efficiency of TiO_2 is restricted by a few factors such as the fast electron-hole recombination and the limited utilization of sun light in visible light range (400-800 nm). Above issues impede its broad applications in energy and environmental areas. Preparation of heterojunctions of core@TiO_2 may induce the transition of the optical response from the UV to visible region, and separate the electrons and the holes into different regions of the catalyst [12, 13]. Alpha-iron oxide (α-Fe_2O_3) is a promising material for catalysis because of its stability, favourable band gap, low cost and abundance [14-16]. The combination of TiO_2 with Fe_2O_3 to form a core-shell structured nanocomposite can decrease the recombination rate of photogenerated electrons and holes. Moreover, the core-shell structured Fe_2O_3@TiO_2 nano-composites can be used to improve the visible light response of TiO_2 [17, 18].

In this study, we demonstrate a facile coating method to fabricate porous 1D α-Fe_2O_3 @TiO_2 core-shell structures by control the condensation of tetrabutyl titanate (TBT) in acetone solution for constructing uniform porous TiO_2 shells. This method is very simple, yet important, which can be extended for coating TiO_2 shells on different cores and allows varying the thickness of TiO_2 shells. In addition, no high temperature calcination is needed for crystallization into anatase phase. Moreover,

the as-prepared 1D α-Fe_2O_3@TiO_2 core-shell structures exhibits highly enhanced photo degradation performance under visible light irradiation.

Experimental

Preparation of α- Fe_2O_3 Particles

In a typical procedure, 6.758 g of $FeCl_3 \cdot 6H_2O$ was dissolved in 250 mL of distilled water to prepare a 0.1 M $FeCl_3 \cdot 6H_2O$ solution. This solution was subsequently heated at 80°*C* for 16 h to obtain akaganeite (β-FeOOH) nanorods. These nanorods were then collected by centrifugation and thoroughly washed with deionized water and 1.0 M NaOH solution several times to remove excess chlorine (Cl) ions and naturally dried at 60℃ for 5 h. Upon drying, the β-FeOOH nanorods were calcined in air at 400 ℃ for 2 h to convert them to porous α-Fe_2O_3 nanorods.

Synthesis of α-Fe_2O_3@TiO_2 core-shell nanoparticles

In a typical procedure, 0.05 mL titanium (IV) butoxide 97% (TBT) was added to 10 mL ethylene glycolate (EG). The mixture was magnetically stirred for 8 h at room temperature, noted as Solution A. 3 mL α-Fe_2O_3 colloidal suspension (0.01 M) was poured into 10 mL acetone under stirring for around 5 min, noted as Solution B. Then, 0.5 mL Solution A was added in Solution B, and left it for ageing 1 h. The precipitates (titanium precursor) were harvested by centrifugation and then dispersed in boiling water for bath ~2 h. The white grey colloids were centrifuged at 3,000 rps for 10 min, then washed with alcohol, and finally dried in vacuum at 60 °C for a few hours to generate α-Fe_2O_3@TiO_2 core-shell particles.

Characterizations

The shape and microstructure was confirmed by TEM (JEOL 1400), operated at an accelerated voltage of 100 kV. The TEM specimen was prepared by dropping solution onto the copper grid and dried in air naturally. The crystalline structure of the composite colloids was further characterized by high resolution TEM (HRTEM), Philips CM200, at an accelerating voltage of 200 kV. To observe surface, SEM (Hitachi 900) was used and operated at 20 kV. To further understand the surface, XPS analysis was conducted with a Physical Electronics PHI 5000 Versa probe spectrometer with Al Kα_radiation (1486 eV). Analysis of the spectra was done using the Physical Electronics Multipak software package. The composition analysis of final products was conducted by XRD (Philip MPD diffractometer) with Cu Kα radiation with scanning step of 2θ= 0.02 °/s. The UV-visible absorption spectrum was obtained on a Shimadzu UV-2600 UV-Vis spectrophotometer (Varian) with a 1-cm quartz cell. The surface area of the as-synthesized powders and pore size distribution were measured by BET equipment (TriStar 3000) via nitrogen gas adsorption and desorption isotherms.

Photocatalysis Test

The photocatalytic activities of TiO_2 based core-shell nanocomposites were determined by measuring the decolourization of methylene blue (MB) under simulated solar light irradiation in a batch reaction. The reactor volume is 250 mL. A 300W xenon lamp (PLS-SXE300C) equipped with AM 1.5G total reflection filters was used to obtain simulated solar light to trigger the photocatalytic reaction, the lamp was positioned about 15 cm away from the reactant solution meniscus. The luminance of the light source over the reactant solution was 0.7 W/cm^2. A 100 mL solution of 30 ppm MB was injected into the reaction system, while 0.020 g of the photocatalyst was added. Prior to irradiation, the suspension was magnetically stirred in the dark for 30 min to ensure adsorption-desorption equilibrium. At given time intervals, 3 mL solution was sampled and filtrated to remove the catalysts. The filtrates were analysed by recording the variations of the absorption band maximum (657nm) of MB using a Shimadzu UV-2600 UV-Vis spectrophotometer. After various time intervals, MB concentration could be estimated using the following equation:

$$\text{MB concentration}=C/C_0\times 100\% \quad (1)$$

Where C_0 is the initial MB absorbance at 657 nm and C is the absorbance obtained after various intervals of time. To eliminate the effect of heating during irradiation, the reactor was equipped with reflux condensation. After decolourization, the supernatant of the solution was obtained via centrifugation, and then characterized by UV-Vis spectroscopy.

Experimental

Morphology and Composition

As revealed by SEM and TEM images in fig. 1A and B, uniform spindle-shaped α- Fe_2O_3 spindle-shaped nanorods were first synthesized with a diameter of ~ 100 nm and length of ~ 400 nm as the cores using hydrothermal method. Then, via a sol-gel process and condensation of titanium glycolate in acetone, uniform core-shell α- Fe_2O_3@TG spindle-shaped structures can be obtained. After water boiling in air, the size of spindle-shaped structures are retained the same, however, as shown in the SEM and TEM image (fig. 1C and D), the surface of the shell become rough. The XRD pattern of the water boiled sample (Fig. 2A) exhibits the characteristic diffraction peaks, which can be well indexed to anatase TiO_2 and α- Fe_2O_3. The XRD pattern of the achieved nanocomposites contains the peaks mainly attribute to α-Fe_2O_3 (JCPDS no.33-0644), a few peaks attribute to TiO_2. This may be caused by the very small weight fraction of the TiO_2 shell, compared with that of the α-Fe_2O_3 cores in the whole core-shell nanocomposites. No other peaks related to impurities are observed, which indicates the high purity of the product. XPS analysis was used to obtain further information regarding the surface structure and composition of the α- Fe_2O_3 @TiO_2 core-shell nanostructures. Fig. 2B shows the characteristic energy peaks of the elemental titanium, oxygen and iron, with binding energies of Eb=459.08 eV (Ti2p), Eb=530.64eV (O1s) and Eb=710.68 eV (Fe2p), respectively. The C1s peak originated form the adventitious carbon. The XPS survey confirms that the TiO_2 shell exists on the surface of the α- Fe_2O_3 particles.

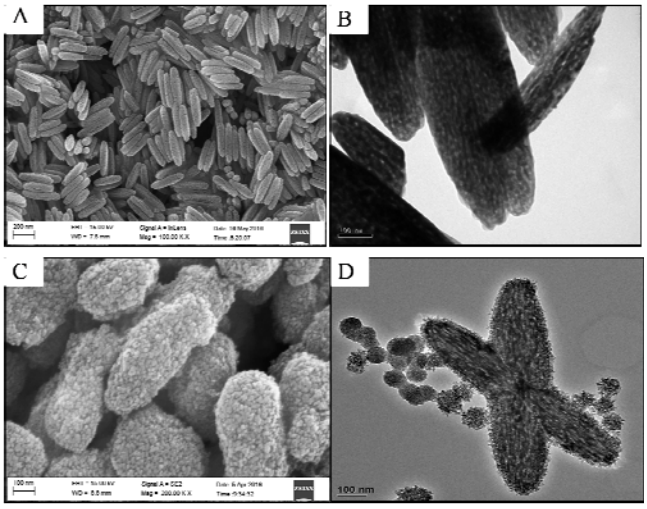

Fig. 1 (A) SEM image of as-preparedα-Fe_2O_3 nanorods; (B) TEM image of α-Fe_2O_3 nanorods; (C) SEM image of α-Fe_2O_3 nanorods coated with TiO_2 nanoparticles; (D) HRTEM image of α-Fe_2O_3@TiO_2 core-shell nanostructure.

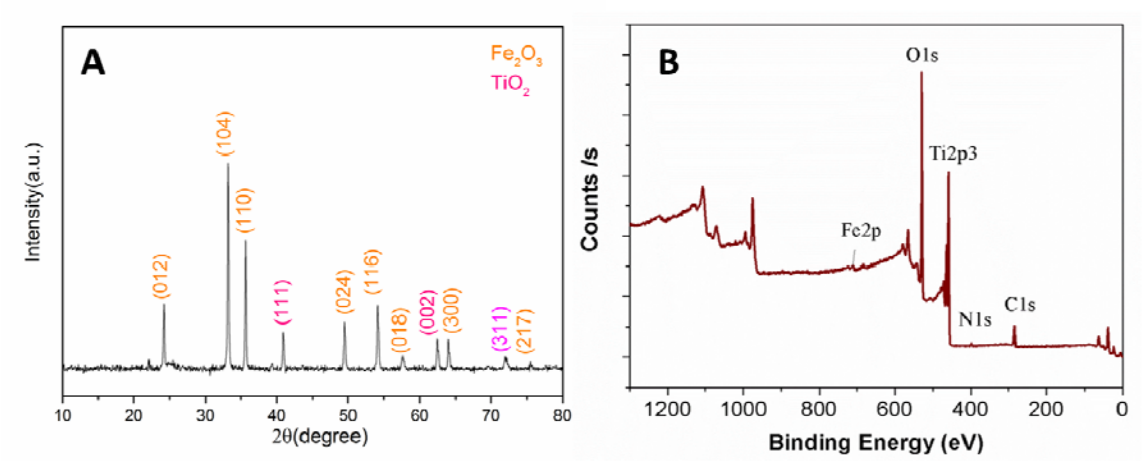

Fig. 2(A) XRD pattern of α- Fe_2O_3 @TiO_2 core-shell nanostructures; and (B) XPS spectra of the as-prepared α- Fe_2O_3 @TiO_2 core-shell nanostructures.

Optical Property

Fig. 3 shows the UV-Vis spectra of pure TiO_2 and α-Fe_2O_3@TiO_2 core-shell nanostructures. For pure TiO_2 particles, the absorption peak appeared at ~320 nm. However, when α- Fe_2O_3 nanorods are coated with TiO_2 nanoparticles, a wide absorption peak appears in the range of 400 nm to 800nm. Comparing with pure TiO_2 particles, it was found that there is an obvious red shift in the absorption peak from UV region to visible light region, which is highly beneficial to enhancing the photocurrent performance and photocatalytic activity of α-Fe_2O_3@TiO_2 core-shell nanostructures under solar light irradiation.

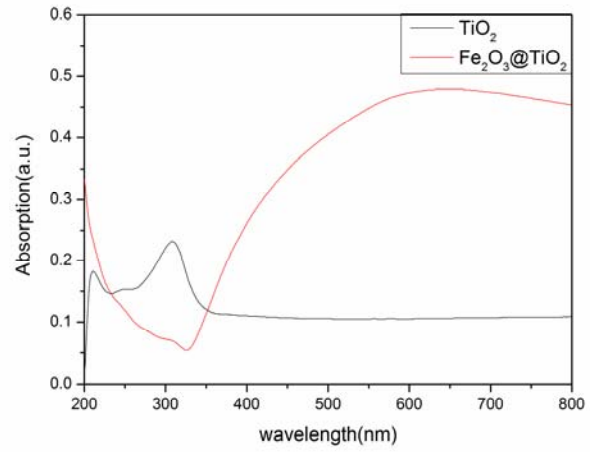

Fig. 3 UV-vis spectra of TiO_2 nanoparticles and α-Fe_2O_3 @TiO_2 core-shell nanostructures.

BET Study

The Brunauer-Emmett-Teller (BET) surface area and pore volume of the as-prepared α-Fe_2O_3@TiO_2 nanocomposites are calculated to be 152m^2/g and 5.8 cm^3/g, respectively. After coating with TiO_2 shells, the BET surface area is greatly increased (The surface area and pore volume of pureα-Fe_2O_3 is 52.5 m^2/g and 8.6 cm^3/g). This results from the densification of TiO_2 networks and the growth of nanocrystals. The corresponding pore size distribution curves (Fig. **4**B) derived from the adsorption branches of the isotherms by using the Barrett-Joyner-Halenda (BJH) method clearly show a smaller pore size than that of the uncoated α- Fe_2O_3 nanorods, further illustrating those small amorphous nanoparticles are aggregated, and grow into large anatase nanocrystals. Such large mesoporosites

derived from the uniform TiO_2 nanoparticles, in association with the very thin layer of TiO_2, are expected to show high performances when they are applied to photocatalytic reactions.

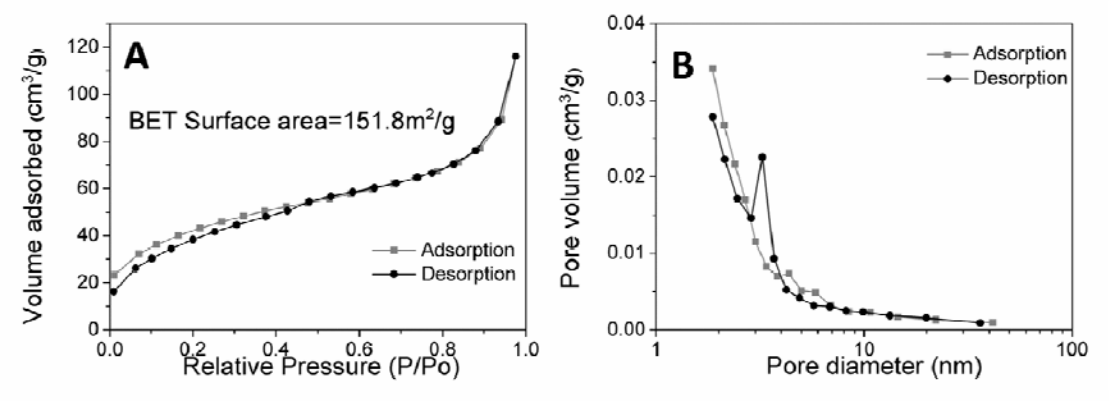

Fig. 4 BET measurements for α- Fe_2O_3 @TiO_2 core-shell nanostructures (A) and (B) with a surface area of S α-Fe_2O_3 =151.8 m^2/g and an average pore size of 5.8 nm.

Photocatalytic Study

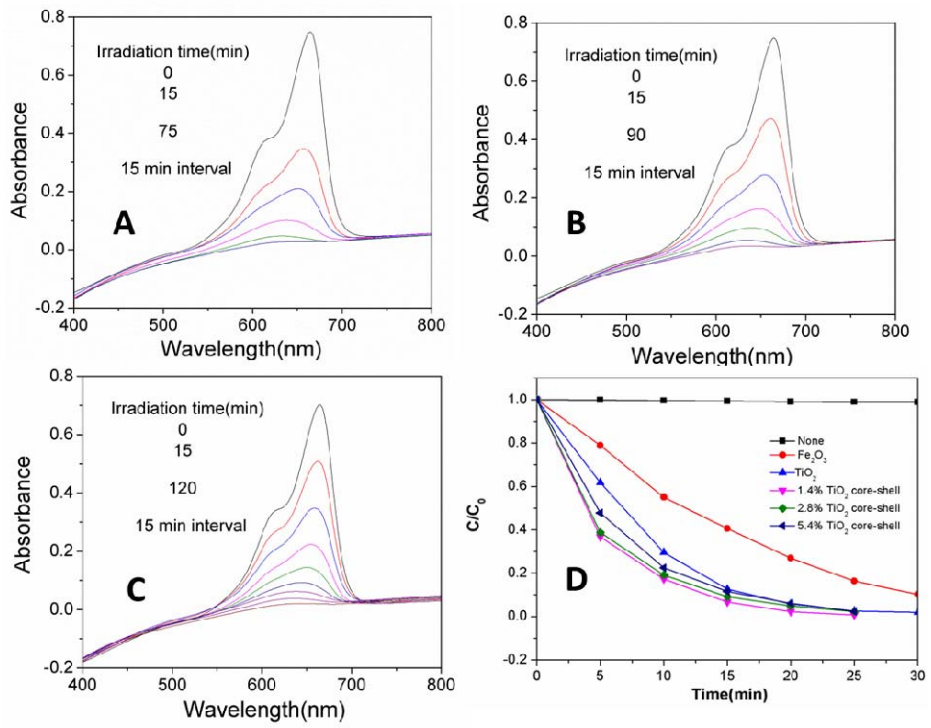

Fig. 5 Absorbance changes of MB molecule during visible light irradiation with different photocatalyst (A) α-Fe_2O_3@TiO_2 core-shell nanocomposites with (A) 1.4% wt. (B) 2.8% wt. and (C) 5.4% wt. TiO_2 coating; (D) Concentration change of MB in the presence of pure TiO_2 nanoparticles, pure α-Fe_2O_3 nanorods and α- Fe_2O_3 @TiO_2 core-shell nanostructures with different TiO_2 coating amount under visible light irradiation.

The photocatalytic performance of the α-Fe_2O_3@ TiO_2 core-shell structures was evaluated by monitoring the degradation of methylene blue (MB) in aqueous solution under UV and visible light irradiation. The organic dye suspension with the photocatalyst was kept in dark conditions for 30 minutes to ensure the establishment of adsorption-desorption equilibrium of MB on the sample surfaces. Fig. 5A-C show the absorbance changes of MB molecular during visible light irradiation with photocatalysts of α-Fe_2O_3@TiO_2 core-shell nanocomposites with (A) 1.4% wt. (B) 2.8% wt. and

(C) 5.4% wt. TiO_2 coating. As can be seen that the core-shell structure with 1.4% wt. TiO_2 coating shows the fastest photocatalytic efficiency, the dye molecular can be totally degraded with 75 min (Figure 5A). Followed with that of 2.8 % wt. TiO_2 coating, nearly 100% degradation can be achieved with 90 mins at the same conditions (Fig. 5B). While the core-shell structure with 5.4% wt. TiO_2 coating shows the slowest degradation rate, fully photo-decomposition happens after 120 mins (Fig.5C). Fig. 5D shows the corresponding concentration changes of the MB solution as a function of visible light exposure time, with the as-prepared pure α-Fe_2O_3, TiO_2 and α- Fe_2O_3@ TiO_2 core-shell structures with different amount of TiO_2 coating as photocatalysts.

MB solution alone without photocatalyst was conducted to test the self-photo degradation of MB. It can be seen that the photocatalytic activity of the α-Fe_2O_3@TiO_2 core-shell structures can be tuned via controlling the coating amount of TiO_2 shells. The thinner the coating is, the faster the visible light photocatalytic activities can be achieved. The visible light photocatalytic performance of all the α-Fe_2O_3@TiO_2 core-shell nanocomposites is superior to that of pure TiO_2 and α-Fe_2O_3.

Under visible light irradiation, TiO_2 is unable to be excited to generate electron-hole pairs, whereas Fe_2O_3 could be activated and yield charge carriers[19]. Subsequently, the photo generated electrons immigrate from the conduction band of Fe_2O_3 to the conduction band of TiO_2 under the action of built-in electric field and the concentration gradient activated and yielded charge carriers, while photogenerated holes accumulated in the valence band of Fe_2O_3. The negative electrons in the conduction band of TiO_2 further react with molecular oxygen O_2 dissolved in the solution to form the superoxide anion O^{2-} and hydrogen peroxide H_2O_2. While the accumulated holes in the valence band of Fe_2O_3 react with OH^- species existing on the surface of the catalyst, producing reactive hydroxyl radicals (·OH), which is the predominant species in the process of photocatalysis .

Conclusion

In summary, the Fe_2O_3@TiO_2 core-shell nanostructures have been fabricated via a simple but efficient synthesis route. This synthesis strategy shows a few advantages in generating anatase TiO_2 shells, such as rapid and effective surface coating, no need of high temperatures (>500°C) treatment. The as-prepared Fe_2O_3@TiO_2 core-shell nanocomposites display a large surface area and high stability. In particular, Fe_2O_3@TiO_2 composites have been proved to show superior visible light photocatalytic activity to the pure TiO_2 nanoparticles and Fe_2O_3 nanorods. The narrow bandgap of Fe_2O_3 was employed to extend the optical response of TiO_2 to visible light. It is shown that the Fe_2O_3@TiO_2 heterojunction structures favours the charge transfer and suppress rapid recombination of photo-induced electrons and holes.

Acknowledgement

We gratefully acknowledge the financial support from the China Postdoctoral Science Foundation (No.2015M581353), National Natural Science Foundation of China (No. 51404066), the National Basic Research Program of China (N150203005).

References

[1]. R. Ghosh Chaudhuri, S. Paria, Core/Shell Nanoparticles: Classes, Properties, Synthesis Mechanisms, Characterization, and Applications, Chem. Rev. 112 (2012) 2373-2433.

[2]. C. J. Zhong, M. M. Maye, Core–Shell Assembled Nanoparticles as Catalysts, Adv. Mater. 13 (2001) 1507-1511.

[3]. F. Caruso, X. Shi, R. A. Caruso, A. Susha, Hollow Titania Spheres from Layered Precursor Deposition on Sacrificial Colloidal Core Particles, Adv. Mater. 13 (2001) 740-744.

[4]. J. Lee, Y. Lee, J. K. Youn, H. B. Na, T. Yu, H. Kim, S.-M. Lee, Y.-M. Koo, J. H. Kwak, H. G. Park, H. N. Chang, M. Hwang, J.-G. Park, J. Kim, T. Hyeon, Simple Synthesis of Functionalized

Superparamagnetic Magnetite/Silica Core/Shell Nanoparticles and their Application as Magnetically Separable High-Performance Biocatalysts, Small. 4 (2008) 143-152.

[5]. Q. Zhang, I. Lee, J. B. Joo, F. Zaera, Y. Yin, Core–Shell Nanostructured Catalysts, Accounts of Chem.l Res. 46 (2013) 1816-1824.

[6]. P. Hu, J. V. Morabito, C.-K. Tsung, Core–Shell Catalysts of Metal Nanoparticle Core and Metal–Organic Framework Shell, ACS Catal. 4 (2014) 4409-4419.

[7]. C. K. Kim, G.-J. Lee, M. K. Lee, C. K. Rhee, A novel method to prepare Cu@Ag core–shell nanoparticles for printed flexible electronics, Powder Tech. 263 (2014) 1-6.

[8]. R.-J. Wu, D.-J. Lin, M.-R. Yu, M. H. Chen, H.-F. Lai, Ag@SnO_2 core–shell material for use in fast-response ethanol sensor at room operating temperature, Sens. Actuators, B: Chemical. 178 (2013) 185-191.

[9]. S. J. Oldenburg, R. D. Averitt, S. L. Westcott, N. J. Halas, Nanoengineering of optical resonances, Chem. Phys. Lett. 288 (1998) 243-247.

[10]. D. W. Manley, R. T. McBurney, P. Miller, R. F. Howe, S. Rhydderch, J. C. Walton, Unconventional Titania Photocatalysis: Direct Deployment of Carboxylic Acids in Alkylations and Annulations, J. Am. Chem. Soc. 134 (2012) 13580-13583.

[11]. S. Liu, X. Fu, Y.-J. Xu, Synthesis of M@TiO_2 *(M = Au, Pd, Pt)* Core–Shell Nanocomposites with Tunable Photoreactivity, J. Phys. Chem. C. 115 (2011) 9136-9145.

[12]. C. Wang, L. Yin, L. Zhang, N. Liu, N. Lun, Y. Qi, Platinum-Nanoparticle-Modified TiO_2 Nanowires with Enhanced Photocatalytic Property, ACS Appl. Mater. & Interfaces. 2 (2010) 3373-3377.

[13]. N. Zhang, S. Liu, Y.-J. Xu, Recent progress on metal core@semiconductor shell nanocomposites as a promising type of photocatalyst, Nanoscale. 4 (2012) 2227-2238.

[14]. J. Zhu, Z. Yin, D. Yang, T. Sun, H. Yu, H. E. Hoster, H. H. Hng, H. Zhang, and Q. Yan, Hierarchical hollow spheres composed of ultrathin Fe_2O_3 nanosheets for lithium storage and photocatalytic water oxidation, Energy & Environ. Sci. 6 (2013) 987-993.

[15]. P. Sun, Y. Liu, X. Li, Y. Sun, X. Liang, F. Liu, G. Lu, Facile synthesis and gas-sensing properties of monodisperse [small alpha]-Fe_2O_3 discoid crystals, RSC Advances. 2 (2012) 9824-9829.

[16]. B. Wang, J. S. Chen, H. B. Wu, Z. Wang, X. W. Lou, Quasiemulsion-Templated Formation of α-Fe_2O_3 Hollow Spheres with Enhanced Lithium Storage Properties, J. Am. Chemi.Soc. 133 (2011) 17146-17148.

[17]. J. Liu, S. Yang, W. Wu, Q. Tian, S. Cui, Z. Dai, F. Ren, X. Xiao, C. Jiang, 3D Flowerlike α-Fe_2O_3@TiO_2 Core–Shell Nanostructures: General Synthesis and Enhanced Photocatalytic Performance, ACS Sustainable Chem. & Eng. 3 (2015) 2975-2984.

[18]. M. Chen, X. Shen, Q. H. Wu, W. Li, G. W. Diao, Template-assisted synthesis of core-shell alpha-Fe_2O_3@TiO_2 nanorods and their photocatalytic property, J. Mater. Sci. 50 (2015) 4083-4094.

[19]. Y. Xia, L. Yin, Core-shell structured [small alpha]-Fe_2O_3@TiO_2 nanocomposites with improved photocatalytic activity in the visible light region, Phys. Chem. Chem. Phys. 15 (2013) 18627-18634.